JOURNAL OF OPTOELECTRONICS AND ADVANCED MATERIALS Vol. 15, No. 11 - 12, November – December 2013, p. 1209 - 1216

Analysis of relaxation processes and low frequency dispersion in waste water

EL GHAOUTI CHAHID[a*], REDDAD EL MOZNINE[a], ABDELLAH ZRADBA[a], ADIL DANI[b], ABDERRAHMANE EL MELOUKY[a], LAILA IDRISSI[b] ; OMAR CHERKAOUI[c], ELHASSAN CHOUKRI[d], DAOUD MEZZANE[d] AIMAD. BELBOUKHARI [d]

[a]*Laboratoire de Physique de la Matière Condensée. Université Chouaib DoukKali, El Jadida, Morocco.*
[b]*Laboratoire de Génie de Procédés et Environnement, FST, Mohammedia .Université Hassan II, Mohammedia, Morocco.*
[c]*Laboratoire de Recherche sur les Matériaux Textile, ESITH, Casablanca, Morocco.*
[d]*Laboratory of the Condensed Matter and Nanostructures LMCN Faculty of Science and Technique FST – Gueliz*

Samples of waste water were taken from three different sites of a river; which is located in an agricultural region " Zemamra"; city El Jadida; Morocco. These wastes water are rejected without any previous treatment and they are used in the irrigation of fields near the river. As a first step; these samples were analysed by the conventional methods for a physicochemical and bacteriological evaluation. This analysis showed the presence of organic and inorganic pollutants in these samples. Furthermore; the electrical and dielectric properties of these samples were investigated in the frequency range 100 mHz to 100 KHz at room temperature. These properties were analysed by using the all electrical and dielectric functions. The results indicate that all samples have similar dielectric behaviour. Two processes of conduction and relaxation have been observed, due to the various organic or inorganic loads in each samples. The analysis of the electrical and dielectric properties of these samples might be used to examine the electrokinetic behaviour of waste water due to the presence of organic and inorganic pollutants.

(Received September 28, 2013; received November 7, 2013)

Keywords: Waste water, Relaxation, Dielectric dispersion, Dielectric permittivity, Electrical conductivity, Water contamination

1. Introduction

The environmental problems have no borders. Inorganic matter, organic matter and Heavy metal contaminated water can be a long-term environmental concern and a potential financial liability to landowners. The toxicity, solubility, and mobility of heavy metals are governed by chemical equilibrium of soil–water systems and are dependent on many factors, including water pH, soil pH, pore fluid chemistry, mineralogy, grain size, etc... Excessive levels of heavy metals can be hazardous to man, animals and plants. Many contaminants have been reported as sources of pollution of soil and ground water, e.g., exhaust, waste water and solid wastes from industrial production, fertilizers and pesticides [1]. Agriculture practices constitute significant non-point sources of metals. The main sources of this type of pollution are impurities in fertilizers, pesticides, refuse derived compost, wood preservatives and corrosion of metal objects like metal roofs and fences [2]. The human activity has increased the concentration of heavy metals in soil, water and air. Sources of pollution of soil and ground water include automobile exhaust, waste water and solid wastes from industrial production, fertilizers and pesticides. Nearly all of these contain heavy metals [3].

Traditional methods of characterizing the contaminated water and involve taking water samples and performing chemical analyses on these samples, which are costly and time-consuming processes. In addition, the risk of samples contamination during sampling, transportation and analysis is always substantial. However, an inexpensive method must be used if the sampling is continuous with time, in order to monitor the diffusion and spreading of contamination, enabling preliminary inspection for chemical changes in the measured samples, related with the pollutants. During the last years there has been considerable interest in the development of efficient methods requires characterization of contaminants in a rapid, non-destructive, and economic way. Dielectric spectroscopy may be a relatively simple and direct means of determining contamination and to understand clay-water and contaminant interaction, so it has been proposed by many researchers as a promising tool and experiments have been carried out to establish the sufficiency of this technique to identify subsurface contamination and its sensitivity to different kinds and concentrations of organic or inorganic pollutants [4]. Electrical spectroscopy offers advantages for studying the effect of physical and chemical treatments on the electrical and structural properties of water (example water hyacinth). These properties provide information and distinct relaxation processes were observed in the permittivity, dielectric loss, electrical loss modulus and conductivity of samples [5]. This technique has been also proposed by many researchers as a promising tool and experiments have been

carried out to establish the efficiency of this technique to identify subsurface and aquatic contamination and its sensitivity to different kind and concentrations of organic or inorganic pollutants [6-9].

The aim of the present work was to monitor the physicochemical and bacteriological as a first step of raw sewage from the city of Zemamra (Morocco).

The behavior relaxation processes and low frequency dispersion is investigated by using the all electrical and dielectric functions.

2. Experimental

Three samples of waste water sites of the river are taken from three different sites. They are denoted (S1); (S2) and (S3). They were selected as follows:

The first sample (S1) was taken from a place where wastewater before reaching the river after crossing a path with a distance close to 300 m.

The second sample (S2) was taken from the place where the waste water coming up to the river.

The third sample (S3) was taken from the place where the waste water is located to the opposite side for sample (S2).

The concentration of the amount of metals in the different samples of waste water were measured at REMINEX; Marrakech; using Inductance Coupled Plasma (ICP). The concentration of the elements present in the tree samples are shown in Table1.

The concentrations of the organic pollution load were determined, at laboratory ESITH, using the physicochemical and biological characterization (electrical conductivity, pH, suspended matter, biochemical oxygen demand and chemical oxygen demand). These physicochemical characteristic of each sample were carried out since September 2011.

The impedance measurement was performed with an electrochemical cell with three electrodes: a saturated calomel electrode (SCE) Ag/AgCl/KClsaturated, used as a reference electrode against a stainless steel electrode and a working electrode in glacier atoms. The three electrodes are connected to an analyzer VoltaLab (radiometer analytical, HIS/HER/ITS) and PGZ301 potenstiostat, a sample holder, a set of coaxial cables, and a personal computer for data processing, a software is used for the receipt of given them, to a polarization of 10 mV and in a domain of frequency that varies from 100 mHz to 100 KHz.

3. Results and discussion

3.1. Inductance Coupled Plasma (ICP) measurements

The amount of metals (mg/l) present in the tree samples are given in Table 1. As seen in Table 1, the concentrations of Na, Mg, Ca, K and P are higher than the limit value of wastewater for irrigation in Morocco. Sodium Na is known for its toxicity to agriculture, we find that the concentration exceeds 50% limit in all samples. The presence of sodium ions with high concentrations is related to the use of fertilizers for soil fertility in the region Zemamra which is known by intense agricultural activity. For against, the concentration of heavy metals remains low in these samples, with the exception of the cadmium (Cd) which has a high rate of 10%. The low content of other heavy metals (Pb, Cr, Mn, Mo and Ni) can be explained by their deposition in the soil. Thus, soil samples from the same location are outstanding analysis by ICP to assess the content of heavy metals.

The total of concentrations of metals (TCM) of the all elements is higher in sample 1. The rank of the increasing of the metal content is as a follow: $\mathbf{S_1 > S_2 > S_3}$

Table 1. Concentration of metals (mg/l) of the tree samples.

Elements	S 1	S 2	S 3	
	% (mg/l)	% (mg/l)	% (mg/l)	*Limit value
Al	1.3	0.2	0.7	5
Cd	0.1	0.1	0.1	0.01
Cr	0.1	0.1	0.1	0.1
Cu	<0.1	<0.1	<0.1	0.2
Pb	0.1	0.1	0.1	5
Mn	0.1	0.1	<0.1	0.2
Mo	0.1	0.1	0.1	0.01
Ni	<0.1	<0.1	<0.1	0.2
Zn	0.2	<0.1	<0.1	2
Fe	1.9	0.3	0.7	5
Ca	94.8	65.5	64	----
Mg	38	31.8	33	----
K	29	11.5	12.1	-----
Na	**464.9**	**487.2**	**329.8**	**9**
P	11.9	3.5	0.6	-----
Li	<0.1	<0.1	<0.1	2.5
Total	**642.5**	**600.5**	**441.3**	

* Quality Standards wastewater

3.2. Physicochemical and bacteriological measurements

The concentrations of the physicochemical and biological, such as suspended matter (SM), chemical oxygen demand (COD) and biochemical oxygen demand (BOD5) are presented in Figures 1 and 2. These figures represent the distribution of concentrations of pollution load in comparison to the limits values; which is attributed by the Moroccan Law for Quality Standards of the wastewater (Law 10 -95 February 4, A1 (No. 2-97-787).

These physicochemical properties of each sample were carried out since September 2011. All sample show high value of the suspended matter (SM) than the limit value of the concentration for the direct reject (50 mg / L) as it is reported by the Quality Standards wastewater.

The concentrations monitoring of (SM) is between 298 mg/L and 472 mg/L for samples 1 and 2. As for

sample 3, the concentrations of suspended matter range from 56 mg/L and 256 mg/L. These values are significantly lower than those of samples 1 and 2. This suggests that amount of theses concentration were deposited in the soil. However; they are still higher than the limit value of direct reject (50 mg/L).

The concentrations of BOD5 is between 212 mg/L and 342 mg/L and of COD between 864 mg/L and 972 mg/L at both samples 1 and 2. While for sample 3, the pollution load may decrease to a value between 12 mg/L and 36 mg/L for BOD5 and a value between 66 mg/L and 120 mg/L for COD. This has a degradation rate of between 10 and 17% for BOD5 and degradation rates between 8 and 13% for COD. Then, the degradation rate varies from 10% to 17% and 8% to 13% for BOD5 and COD respectively and that due to the natural language. Pollutant load remains high compared to the direct reject limit value. In conclusion, the natural language is insufficient and we can speak of an intense pollution and dangerous situation, hence the need to set up an emergency treatment facility.

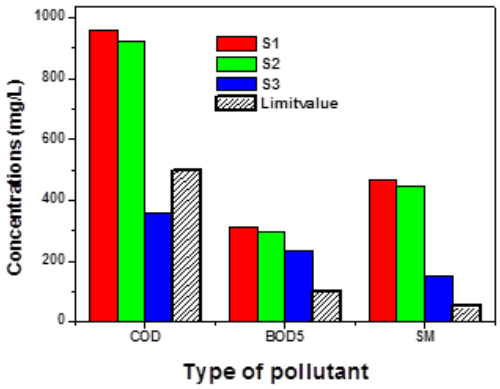

Fig. 1. The distribution of concentrations of COD, BOD5, SM and the total concentrations of the metal elements (TCM) (at Month 09/2011).

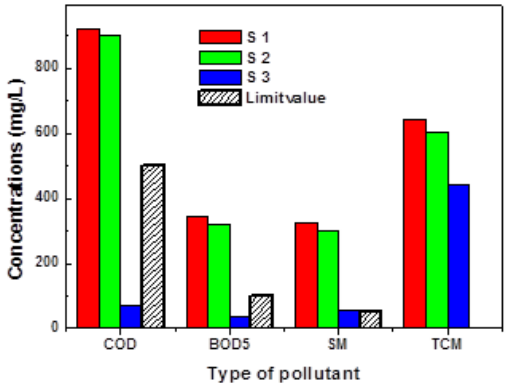

Fig. 2. The distribution of concentrations of COD, BOD5, SM and the total concentrations of the metal elements (TCM) (at Month 07/2012)

4. Dielectric measurement

4.1. Complex dielectric function spectra

Figs. 3 (a) and 3 (b) show the frequency dependence of real (ε') and imaginary part (ε'') of the complex permittivity of different samples. Similar behavior can be observed in alls samples .Both figures show that the dielectric permittivity of the samples decreases with increasing frequency at low frequencies. A high frequency both dependencies show a strong relaxation. However, the dielectric permittivity of the wastewater increases moving from the most polluted area (Sample 1 to sample 3). This behavior is attributed to an increase in the concentration of the pollutant load (existing metal ions in waste water) from the most polluted to less polluted area. The same behavior has been observed due to higher concentrations of leachate at low frequencies where ε' and ε'' increase with the increase in conductivity [10].

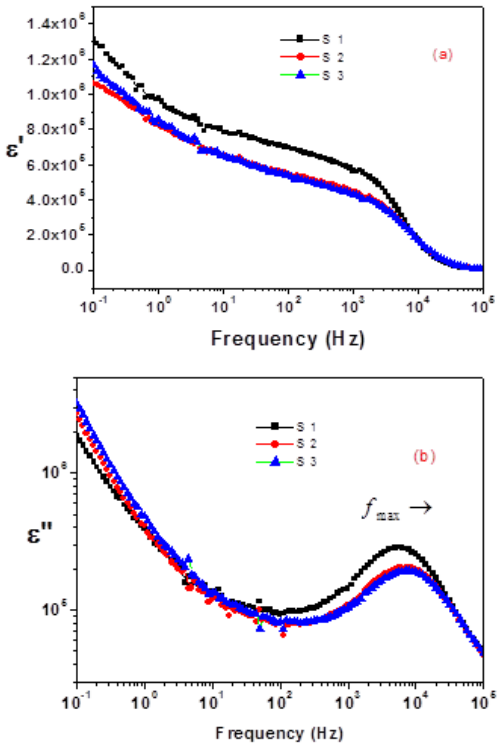

Fig. 3. Frequency dependence of real ε'(a) and imaginary part ε'' (b) of complex permittivity of different samples.

All samples show a significant increases in (ε') and (ε'') in the lower frequency side of the spectra; which is mainly due to the contribution of the electrode polarization (EP) [11-15]. In the higher frequency side of the spectra; the imaginary part (ε'') show a peak indicating a relaxation of Maxell –Wagner (MW).

The EP phenomena occurs due to formation of electric double layer (EDL) capacitances by the free charges build up at the interface between the electrolyte

and the electrode surfaces in plane geometry [16, 17]. Whereas in case of MW phenomena, the free charges build up at the interfacing boundaries of various components of different dielectric constant in the composite dielectric material, which results the nanocapacitors of spherical geometry [17–20]. In EP region, the logarithmic slope of frequency dependent ε values of the dielectric materials closer to –1 indicate leakiness of the EDL capacitances (blocking layers) to moving charges, whereas value close to 0 suggest a complete block of charge movement through the layers [21-24]. The slope of the $\varepsilon(f)$ spectra (Fig. 3) of the investigated sample close to –1 witch suggest the leakiness behavior of the EDL capacitances formed in the EP region.

Indeed; the permittivity of a material is a measure of the extent of distortion of its electric charge distribution in response to an electric field. The main mechanism for dielectric behavior at microwave frequencies (MHz-GHz) is orientation of polar molecules in the presence of an applied alternating electric field [25]. At low frequencies (Hz-MHz), the primary mechanism for a permittivity or an impedance response is the perturbation of charges at the solution-solid interface. Very high permittivity values [26] result from two mechanisms: (i) polarization of the counter ions in the diffuse double layer (DDL), and (ii) the Maxwell-Wagner (MW) that arises from polarization of the charge created by contact of phases with different permittivity.

The application of an electric field causes counter ions in the DDL of charged colloid particles (clay or organic matter (OM)) to move along the surface in response to the electric gradient. The motion is mostly tangential along the surface because of the existence of a much larger energy barrier normal to the surface [27]. Consequently, electric charges accumulate at particle interfaces such as particle edges and water-air interfaces. When the field is removed, the charges relax back to their original distribution by diffusion [28].

4.2. Electric modulus spectra

Generally the complex permittivity format (as shown in fig.3 is used to present most dielectric relaxation phenomena [29]. Occasionally, the complex impedance formalism $(Z(\omega))$ and much less frequently the modulus formalism $(M(\omega))$ are used to present dielectric relaxation behavior. Kyritis et al [30] employed all three presentation formats to analyze the dielectric properties of poly(hydroxyethyl)acrylate/water hydrogels, while Gerhardt [31] showed that the electrical relaxation phenomena in ionic conductors could be better analyzed in the impedance format rather than the admittance format. Provided the dielectric measurements are performed in the linear response regime of the material, it follows that the $\varepsilon^*(f)$ and the $M^*(f)$ formalisms contain the same information. The dielectric modulus is the reciprocal of the complex permittivity, and can be expressed as [32].

$$M^*(\omega) = M'(\omega) + jM''(\omega) = \frac{1}{\varepsilon^*(\omega)} = \frac{\varepsilon'(\omega) + j\varepsilon''(\omega)}{\left[\varepsilon'(\omega)\right]^2 + \left[\varepsilon''(\omega)\right]^2} \quad (1)$$

The two formats differ in terms of how each will highlight, or conversely suppress, the observation of dielectric phenomena. For example, highly capacitive phenomena are suppressed in $M(f)$ plots, particularly when the ratio of the static to the infinite permittivity is high. It follows that a large LFD will be suppressed and any high frequency relaxation amplified (in the relative sense).

Consequently, it seemed interesting to examine the modulus format of the observed spectra, in order to isolate the weak dispersion observed in the permittivity plot.

Frequency dependencies of M' and M'' are shown in Figures 4(a), 4(b) of the alls samples. As it can be seen; the real part of the modulus M' tends to the constant value M'_{∞} at high frequencies; whereas M'' exhibits a peak at low frequency. The value of M''_{max} increases and shifts towards higher frequencies. This shift indicates a relaxation of conductivity in the alls samples. These behaviors indicate that the constitutions of wastewater show a wide variety of frequency-dependent effects associated with their heterogeneity.

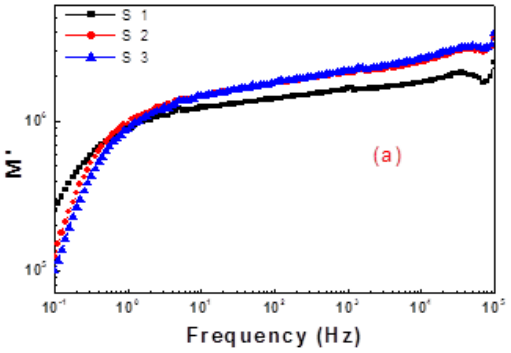

Fig.4.a. Frequency variation of real part of electrical modulus M' of different samples.

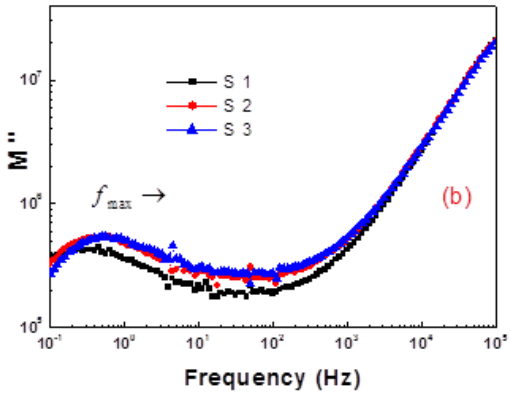

Fig.4.b. Frequency variation of imaginary part of electrical modulus M'' of different samples.

By using the modulus format, it is possible to suppress the visualization of the large contribution of the low frequency dispersion that is otherwise significant in the $\varepsilon''(f)$ plot (fig. 3). The peak in the modulus presentation $M''(f)$ can be seen clearly and confirms the existence of the 'hidden' process in the imaginary part $\varepsilon''(f)$ of the complex permittivity. The modulus format therefore facilitated greatly the visualization of this otherwise 'hidden' process [29].

4.3. Complex impedance spectra

The use of the function Z^* is particularly appropriate for the conductive analysis, whereas M^* and ε^* formalisms are suitable when localized relaxation dominates. Therefore it seem important to analysis also the impedance response. The frequency-dependent can separate these constitutions from their electrical behavior. The complex impedance Z^* is related to the complex permittivity and it is defined by:

$$Z^* = Z' - jZ'' = \frac{1}{j\omega C_0 \varepsilon_r^*} \quad (2)$$

$$\varepsilon^*_r = \varepsilon'_r - j\varepsilon''_r \quad (3)$$

where $\omega = 2\pi f$ [Hz] (f is the frequency); $C_0 = \frac{\varepsilon_0 S}{e}$ is the vacuum capacitance having the same electrodes surface S, the thickness e and the permittivity ε_0.

The variation of the real and imaginary parts of impedance Z' and Z'' as a function of frequency is shown in Figures 5(a), 5(b). It follows that the magnitudes of Z' and Z'' decrease with increase of the frequency. Such behavior indicates the increasing of the ac conductivity and the frequency dependence of the relaxation time. The large value of Z' at low frequency is caused by the electrode polarization. As the amount of pollutant charge increases (From sample 1 to sample 3) the magnitude of Z' decreases and the peak Z''_{max} shifts towards the higher frequencies.

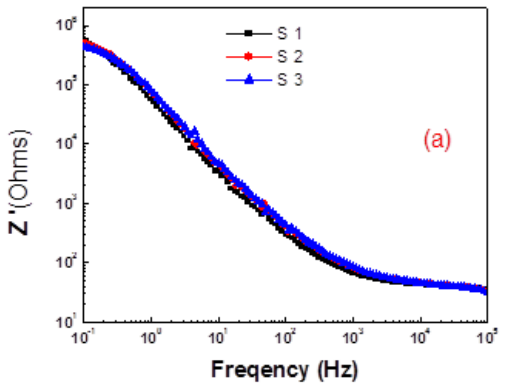

Fig.5a. Frequency dependence of real part Z' (a) of impedance of different samples.

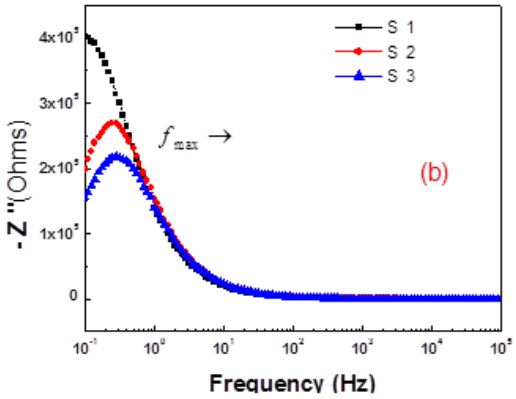

Fig.5.b. Frequency dependence of imaginary part Z'' (b) of impedance spectroscopy at different samples.

In Fig. 6, we reported the evolution of imaginary part Z'' as a function of the real part Z' of different samples (Nyquist plot). We can observe that the increase in the concentration of the polluting load of the waste water results in a decrease of the diameter of the half-circles due to variation of the conductivity produced by the amount of ionic charges existing in the waste water of each sample. The approximate form is a semicircle, characteristic of the association of a resistance in parallel with a capacity. It is worthy that the semicircular decreases when increasing pollution load of waste water, which characterizes a decrease of the resistance in parallel which is associated to the capacitance.

The semi-circles are not perfect but skewed (inclined) with their centers depressed below the real Z' axis. This behavior indicates the presence of non-Debye type relaxation phenomena caused by a distribution of relaxation time [36].

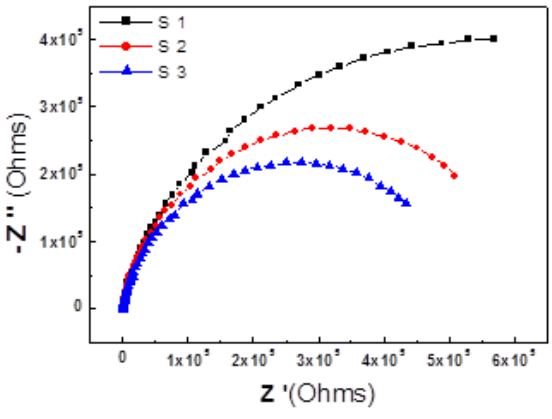

Fig.6. Nyquist plot, imaginary part Z'' as a function of the real part Z' of different samples.

4.4. AC conductivity spectra

The evolution of the $\sigma'(\omega)$ as a function of frequency of all sample is shown in Figure 7. As it can be seen; a plateau at low frequencies and dispersion at high frequencies followed by another plateau. The plateau region corresponding to dc conductivity is found to be extended to higher frequencies when the pollutant charge increases. AC conductivity dispersion takes place at a frequency known as hopping frequency that increases with increasing the amount of the pollutant charge.

It is known that in an electrolyte the electrical conductivity σ is given by the relation:

$$\sigma = \sum n_i \mu_i q_i \quad , \qquad (4)$$

where n_i , μ_i and q_i are the charge carrier density, ionic mobility, and ionic charge of *ith* ion respectively [17].

where n_i , μ_i and q_i are the charge carrier density, ionic mobility, and ionic charge of *ith* ion respectively [17].

The increase of ionic conductivity of a complex system is due to the increment of the number of mobile charge carriers introduced/produced in the material with the change in concentration of the constituent. The dynamical behavior of these samples is governed by the electrical conductivity of organic-inorganic pollutants existing in the waste water of each sample [33].

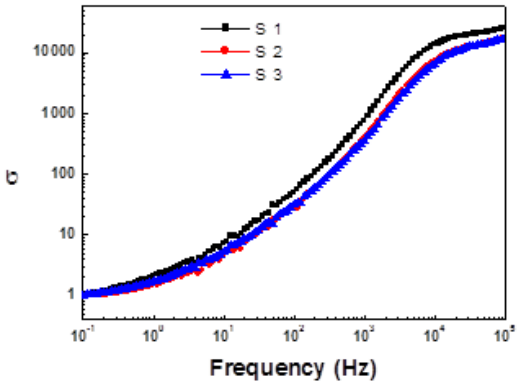

Fig.7. frequency dependence of electrical conductivity σ at differents samples. Normalized to it's initial value.

5. Correlation between relaxation times and the concentration of pollutants.

As it was shown in Figure 7, the electrode polarization effects often do not mask the features of the spectra, owing to suppression of high capacitance phenomena in $M(f)$ plots as it was shown in Fig.4. Therefore; the $(M''(f))$ spectra has the peak value corresponding to the electrode polarization (EP) relaxation frequency f_{EP}, which is used to evaluate the EP relaxation time $\tau_{EP} = (2\pi f_{EP})^{-1}$ [13–16, 22, 34–36].

The correct value of f_{EP} corresponding to the peaks; the maximum $(M''(f))$ spectra in these samples were determined from experimental data.

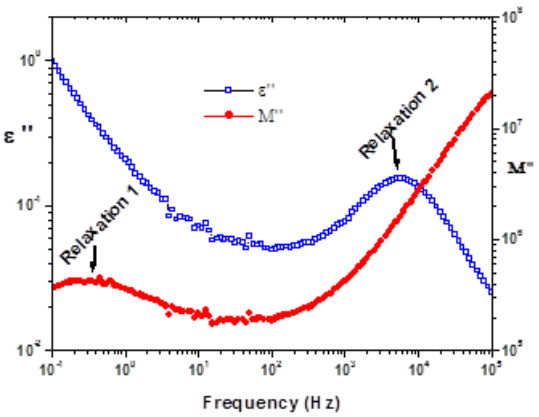

Fig.8. Relaxation in imaginary parts of permittivity $(\varepsilon''(f))$ and modulus $(M''(f))$ versus frequency for sample 1.

Concerning the relaxation behavior as shown in figure 3b; the correct value of τ_P to peaks; the maximum imaginary part (ε'') of the complex permittivity of different samples were determined from experimental data.

These values were reported in table 2.

Table .2. Various of the experimental relaxation time of permittivity τ_P and of modulus τ_M .

Samples	τ_P (s)	τ_M (s)
S 1	2.83E-05	0.36
S 2	2.52E-05	0.25
S 3	2.01E-05	0.20

The rank order for increasing relaxation time (Sample 3 < Sample 2 < Sample 1). This means that a fast relaxation process has occurred in sample 3; followed by sample 2 and sample 1; which show slower relaxation process. At this point, it is interesting to compare the relaxation times and the concentration of amount of the pollutant present in sample.

Relaxation times (τ) and the concentration of the pollutants charge for all samples are presented in fig.9 and fig.10. As it can be seen; for any kind of the pollutant charge; the sample 1 show always the slower process compared to the others sample. This behavior can be explained by the dynamical behavior of organic-inorganic pollutants existing in the waste water [36]. In sample with high amount of the pollutant; there is a greater probability that the cations will be trapped by the ionized organic

product; if the concentration of these charge sites is higher. Therefore, the presence of the ionized organic products reduces the mean diffusion path length and explains the shorter relaxation times observed for the more polluted sample.

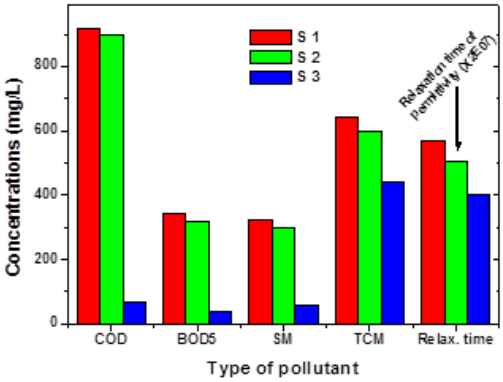

Fig. 9. The distribution of concentrations of COD, BOD5, SM and the total concentrations of the metal elements (TCM) in comparison with the relaxation time from the permittivity (Relax.Time).

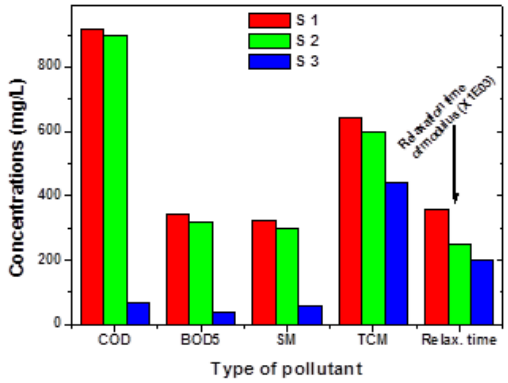

Fig. 10. The distribution of concentrations of COD, BOD5, SM and the total concentrations of the metal elements (TCM) in comparison with the relaxation time from modulus (Relax.Time).

6. Conclusion

The evaluation of physicochemical and bacteriological showed the presence of organic and inorganic pollutants in these samples. The amount of these pollutants is out of the limit values required for the irrigation. Excessive levels of these pollutants can be hazardous to man, animals and plants. The results indicate that all samples have similar behaviour of dielectric and electrical properties. Two processes of the conduction and relaxation have been observed, due to the presence of organic and inorganic pollutants in each samples of the waste water. In sample with high amount of the pollutant; there is a greater probability that a cations will be trapped by the ionized organic product; if the concentration of these charge sites is higher.

The results of this study indicate might be used to characterize the electrokinetic behavior such as diffusion and relaxation related to the physicochemical changes in waste water.

Significant differences in dielectric relaxation kinetics and were observed for the different samples, which were found to correlate with the amount of pollutant present in each sample. The dielectric response was shown to be especially sensitive to the amount of pollutant present in each sample.

Further works are in process to model the behavior of electrical and dielectric of this sample; using an equivalent circuit for a quantitative analysis of each dielectric spectrum, and or using Cole-Cole relaxation model to describe the relaxation processes; where this latter is more appropriate for such system.

In the same time; other soil samples were taken (in the same specific locations where the waste water). They are under investigation in order to evaluate the concentration of organic and nonorganic pollutants as a contaminants.

The dielectric properties of these soil samples are also needed to analysis the behavoiur of organic and nonorganic pollutants.

References

[1] H. M. A. Al-Mattarneh, L. M. Sidek, R. M. A. Ismail, M. F. M. Zain, M. R. Taha, , Dielectric Dispersion Characteristics of Sandy Soil Contaminated by Pb and Cd ; ICCBT 2008 - D - (42) 463 (2008).

[2] B.J. Alloway, 1995. Soil Processes and the behavior of Metals. In: Heavy Metals in Soil. Edited by: B.J. Alloway, Blackie Academic & Professional, London.

[3] M. Fic, M.I. Schroter, Journal of contaminated Hydrology, **4,** 69 (1989).

[4] T. L. Chelidze, Y. Gueguen, Theoretical models, Geophys. J. Int. **137**, 1 (1999).

[5] Medhat Ibrahim, Ragab Mahani, Osama Osman, Traugott Scheytt Open Spectroscopy Journal, **4**, 32 (2010).

[6] A. Kaya, H. Fang, Journal of Environmental Engineering, ASCE, **123**(2), 169 (1997).

[7] A. Kaya, Turk J Engin Environ Sci **25,** 345 (2001).

[8] R. K. Rowe, J. Q. Shang, Y. Xie, Canadian Geotechnical Journal, **38**, 4980 (2001).

[9] J.Q. Shang, W. Ding, R .K. R owe, L. Josic, Can. Geotech. J. **41,** 1054 (2004)

[10] V. Saltas, F. Vallianatos, P. Soupios, J.P. Makris, D. Triantis, Journal of Hazardous Materials, **142**(1–2), 520 (2007).

[11] D. K. Pradhan, R. N. P. Choudhary, B. K. Samantaray, Express Polymer Letters, **2**, 630 (2008).

[12] N. Shinyashiki, R. J. Sengwa, S. Tsubotani, H. Nakamura, S. Sudo, S. Yagihara, The Journal of Physical Chemistry A, **110**, 4953 (2006).
[13] R. J. Sengwa, S. Sankhla, Colloid and Polymer Science, **285**, 1237 (2007).
[14] R. J. Sengwa, S. Sankhla: Journal of Macromolecular Science Part B: Physics, **46**, 717 (2007).
[15] R. J. Sengwa, S. Sankhla, Indian Journal of Engineering and Materials Sciences, **14**, 317 (2007).
[16] R. J. Klein, S. Zhang, S. Dou, B. H. Jones, R. H. Colby, J. Runt, The Journal of Chemical Physics, **124**, 144903 (2006).
[17] J. R. MacCallum, C. A. Vincent: Polymer electrolyte reviews, vol 1. Elsevier, London (1987).
[18] A. Kyritsis, P. Pissis, Macromolecular Symposia, **119**, 15 (1997).
[19] N. Noda, Y-H. Lee, A. J. Bur, V. M. Prabhu, C. R. Snyder, S. C. Roth, M. McBrearty, Polymer, **46**, 7201 (2005).
[20] A. A. Garrouch, H. M. S. Lababidi, R. B. Gharbi, The Journal of Physical Chemistry, **100**, 16996 (1996).
[21] F. Kremer, A. Schnhals: Broadband dielectric spectroscopy. Springer, Berlin (2002).
[22] P. Pissis, A. Kyritsis: Electrical conductivity studies in hydrogels. Solid State Ionics, **97**, 105 (1997).
[23] D. Q. M. Craig, J. M. Newton, R. M. Hill, Journal of Material Science, **28**, 405 (1993).
[24] D. Q. M. Craig, S. A. Barker, D. Banning, S. W. Booth, International Journal of Pharmaceutics, **114**, 103 (1995).
[25] M. V. Burmistr, K. M. Sukhyy, V. V. Shilov, P. Pissis, A. Spanoudaki, I. V. Sukha, V. I. Tomilo, Y. P. Gomza, Polymer, **46**, 12226 (2005).
[26] M. L. Auad, S. R. Nutt, V. Pettarin, P. M. Frontini, Express Polymer Letters, **1**, 629 (2007).
[27] M. Pannirselvam, A. Genovese, M. C. Jollands, S. N. Bhattacharya, R. A. Shanks, Express Polymer Letters, **2**, 429 (2008).
[28] J. Fritzsche, A. Das, R. Jurk, K. W. Stckelhuber, G. Heinrich, M. Klüppel, Express Polymer Letters, **2**, 373 (2008).
[29] R .El Moznine, G. Smith, E. Polygalov, P. M. Suherman, J. Broadhead, J. Phys. D: Appl. Phys. **36,** 330 (2003).
[30] A. Kyritsis, A. Pissis, J. Grammatikakis, J. Polymers Sci. B: Polymer Phys. **33,** 1337 (1995).
[31] M. Gerhardt, J. Phys. Chem. Soilds **55**, 1491 (1994).
[32] A, Jonscher, , J. Phys. D: Appl. Phys. **32,** R57 (1999).
[33] Y. Mamunya, A. Kanapitsas, P. Pissis, G. Boiteux, E. Lebedev, Macromolecular Symposia, **198**, 449 (2003).
[34] S. Zhang, S. Dou, R. H. Colby, J. Runt, Journal of Non-Crystalline Solids, **351**, 2825 (2005).
[35] R. J. Sengwa, S. Sankhla, Polymer, **48**, 2737 (2007).
[36] R. J. Sengwa, S. Sankhla, Polymer Bulletin, **60**, 689 (2008).

*Corresponding authors: chahidoo@yahoo.fr; elmoznine@yahoo.fr